# Evaluation of Some Recent High Degree Geopotential Harmonic Models in Egypt

***Dr. Maher Mohamed Amin***

*Lecturer of Surveying, Surveying Department, Shoubra Faculty of Engineering, Zagazig University*

**Abstract:**

Recently, several high and ultra-high degree global harmonic models have been developed. They are typically used in local gravity field modeling via the remove-restore technique, in order to establish accurate and precise local geoid solutions. In the current study, a comparison is performed, concerning Egypt, among the behaviors of the new harmonic models EGM96, GFZ97 and GPM98C with respect to the available local data. These comparisons ascertain that none of these new models recover the long-medium spectral information in a reliable manner, due to the absence of the Egyptian local data during the global solutions for those harmonic models. Among the three investigated harmonic models, the EGM96 model, as a reference field, seems to perform slightly better than the other two models, based on the available Egyptian data set. So, it is recommended to improve the EGM96 model, using the local Egyptian data.

## 1 Introduction

Gravimetric geoid modeling is usually performed using an Earth geopotential model along with a set of detailed local data (Amin, 1983). Therefore, the existence of a high-quality geopotential model that fits the local gravity field is necessary for the determination of an accurate and precise gravimetric local geoid. Advances in satellite dynamic techniques, terrestrial gravimetry, satellite altimetry and solution methods have led to the development of many new global harmonic models. However, the highest resolution and precision achievable for a global harmonic model is constrained by the coverage, resolution and accuracy of the available terrestrial data over the entire globe.

In Egypt particularly, the application of the global geopotential models is problematic. Some previous studies have been made to test the validity of a group of earlier models that date back to the eighties and the beginning of the nineties, e.g. (Hanafy, 1993 and El-Tokhey, 1995). They concluded that the absence of the local data from the global data set, used for the solution of such models, reduces the benefit of using these models in local geoid modeling for Egypt.

Since none of the new models have been tested for the same local region tell now, it is therefore justified to try once more testing some of these recent global models to detect whether or not the local Egyptian data has been supplied to any of these global models, and to choose the model that best fits the gravity field in Egypt. Hence, the purpose of this paper is to further investigate the actual performance of three of the recent versions of such harmonic models, regarding Egypt. A thorough comparison is held among these high-degree models, concerning their local behavior and performance in Egypt. Finally, conclusions and recommendations are drawn.

2002, *Port-Said Engineering Research Journal PSERJ, Vol. 6 No.(2), Published by Faculty of Engineering, Suez Canal University, Port-Said, Egypt*

## 2 The geopotential models under study

The geopotential models under investigation are the EGM96 complete to degree and order 360 (Lemoine et al., 1996), the GFZ97 complete to degree and order 359 and the GPM98C harmonic model(Wenzel, 1998), truncated at degree and order 720. EGM96 is a very well globally established high degree harmonic model that was selected as the final product out of five NASA/GSFC preliminary test models. These five test models were checked regarding their local performances as reference fields in different selected areas all over the world (Smith and Milbert, 1997). In addition, the EGM96 harmonic coefficients (along with their standard errors) are completely available to the geodetic community, with a sufficiently large numerical accuracy.

The GFZ97 model represents the recent improved version of the GFZ-harmonic model series (Gruber et al., 1997). However, the GFZ97 coefficients (as well as their error estimates) are released with a considerably smaller numerical accuracy, compared to those pertaining to the EGM96 model. GPM98C is an ultra-high degree geopotential model originally computed to degree and order 1800. However, it is available only up to degree and order 720 and the coefficients' standard deviations are not given.

Both the EGM96 and GFZ97 harmonic models are high-degree combined solutions, which are based on satellite dynamics observations, satellite altimetry and global terrestrial gravimetry. GPM98C is a globally extended (ultra-high degree) harmonic model that had as input updated global 5'x5' mean free air anomaly data, new satellite altimetry data and EGM96 as a reference model. Wenzel (1998) states that GPM98C would not have a better performance than EGM96 in areas, which had no newer local data contribution to the GPM98C.

## 3 The low frequency geoid features in Egypt pertaining to the three models

The models under consideration were used for computing the respective low degree geoids, relative to the WGS-84 reference ellipsoid, at the nodes of a 5'x5' grid covering Egypt ($22°N \le \varphi \le 32°N$; $25°E \le \lambda \le 36°E$). These computations utilized the well known spherical harmonic series

$$N_{Model} = (GM/r\gamma) \sum_{n=2}^{Nmax} (a/r)^n \sum_{m=0}^{n} (\bar{C}^{*}_{nm} \cos m\lambda + \bar{S}_{nm} \sin m\lambda) \bar{P}_{nm}(\sin\theta), \quad (1)$$

with

$\theta$ the geocentric latitude,
$\lambda$ the geodetic longitude,
$r$ the geocentric radius to the geoid,
$\gamma(\theta,r)$ the normal gravity induced by the WGS-84 reference ellipsoid,
$GM$ the Earth mass-Gravitational constant product consistent with the harmonic model's coefficients,
$a$ the equatorial radius scale factor associated with the model,
$\bar{C}^{*}_{nm}$ the relevant fully normalized spherical harmonic C-coefficients of degree n and order m, reduced for the even zonal harmonics

of the WGS-84 reference ellipsoid,

$\bar{S}_{nm}$ the relevant fully normalized spherical harmonic S-coefficients of degree n and order m,

$\bar{P}_{nm}(\sin\theta)$ the fully normalized associated Legendre function of degree n and order m,

Nmax the maximum degree of the respective harmonic model.

Table (1) illustrates the statistics of the resulting harmonic models' geoid grids and of the differences among the relevant pairs of geoids. In addition, Figure (1) through (6) show the corresponding contour maps. From Table (1) and Figures (1), (3) and (5) it is clear that, regarding Egypt and as expected, there exists a small difference between the EGM96 and the GPM98C low frequency behavior, expressed in the small difference between the respective two geoids. These differences have a small standard deviation. Also, Table (1) and Figures (1), (2), (3), (4) and (6) show that there is a considerable larger differences between both the EGM96 & GPM98C harmonic models and the GFZ97 model. However, from Table (1) it is clear that (at some point) an absolute difference of at least 2 meters could occur between any pair of models.

**Table (1): Statistical comparison among the 5'x5' geoid grids computed from the different harmonic models (Unit: meters)**

| Item | Mean | Std. Dev. | RMS | Min. | Max. |
|---|---|---|---|---|---|
| EGM96 geoid | 13.804 | 2.691 | 14.064 | 7.532 | 21.143 |
| GFZ97 geoid | 13.488 | 3.066 | 13.832 | 6.938 | 21.650 |
| GPM98C geoid | 13.806 | 2.687 | 14.065 | 7.125 | 21.100 |
| EGM96-GFZ97 geoid | 0.316 | 0.668 | 0.739 | -1.566 | 2.849 |
| EGM96-GPM98C geoid | -.002 | .229 | .229 | -1.500 | 2.046 |
| GFZ97-GPM98C geoid | -0.318 | 0.706 | 0.774 | -2.800 | 1.877 |

## 4 The statistical fit of the investigated models with the local data

In order to investigate the long-to-medium wavelength contribution of the harmonic models with respect to the local data (Shaker et al., 1997), the gravity anomaly contributions of the three models were subtracted (removed) from the available Egyptian free air anomaly data. In addition, the geoid components of the models were removed from the available geoidal height observations at GPS-benchmarks. The available GPS-benchmarks are 80 points, which are well distributed over the Egyptian territory. Of course, the geoid contributions of the harmonic models were computed using Eq. (1) at the relevant (scattered) points. The gravity anomaly components of the models were analogously assessed as follows

$$\Delta g_{Model} = (GM/r^2) \sum_{n=2}^{Nmax} (n-1)(a/r)^n \sum_{m=0}^{n} (C^*_{nm} \cos m\lambda + \bar{S}_{nm} \sin m\lambda)\, \bar{P}_{nm}(\sin\theta) \qquad (2)$$

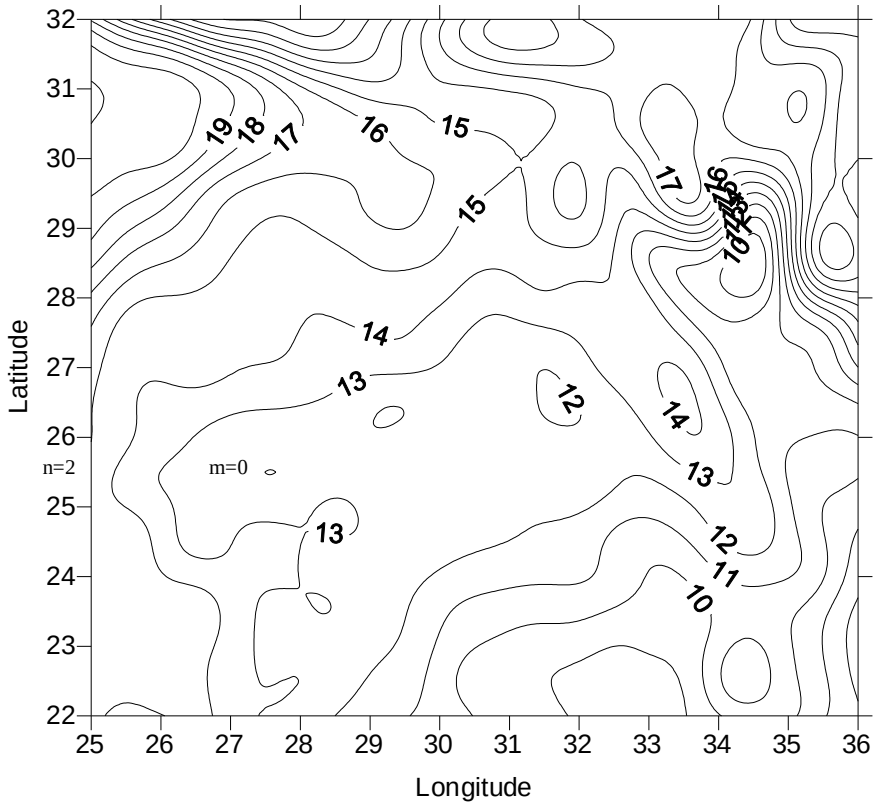


**Figure (1): Contour map of the EGM96 geoid for Egypt (Interval: 1.0 m)**

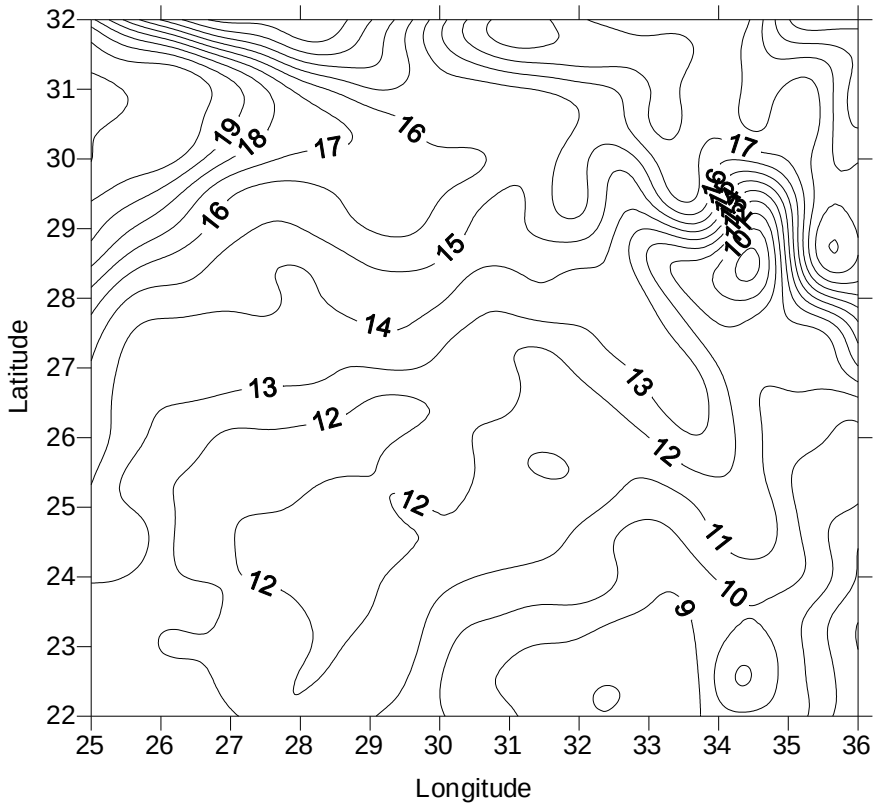


**Figure (2): Contour map of the GFZ97 geoid for Egypt (Interval: 1.0 m)**

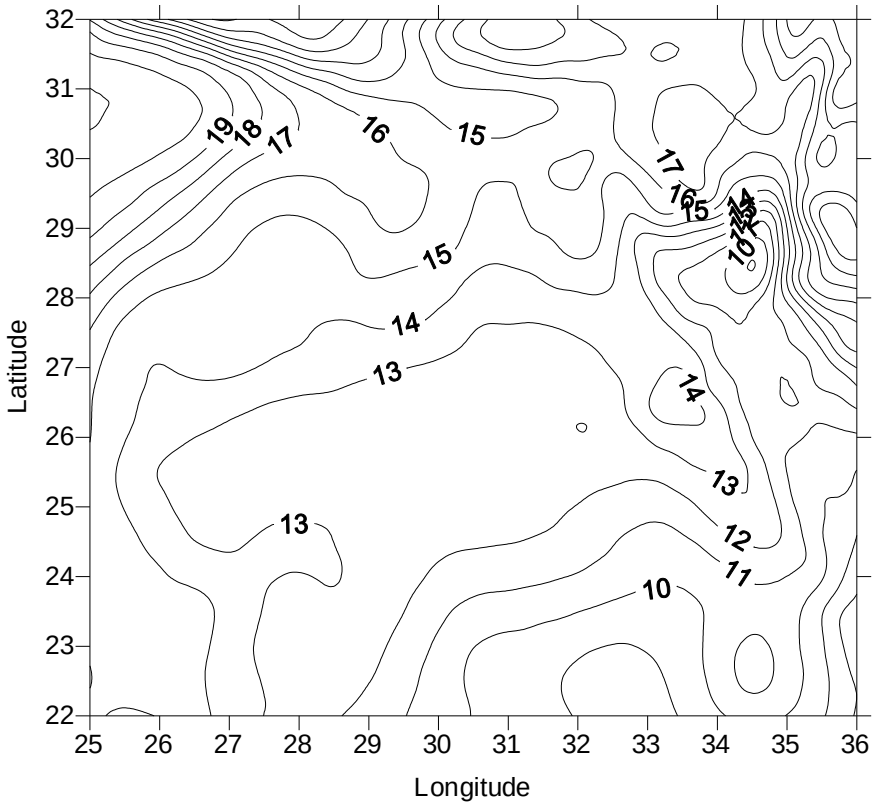


**Figure (3): Contour map of the GPM98C geoid for Egypt (Interval: 1.0 m)**

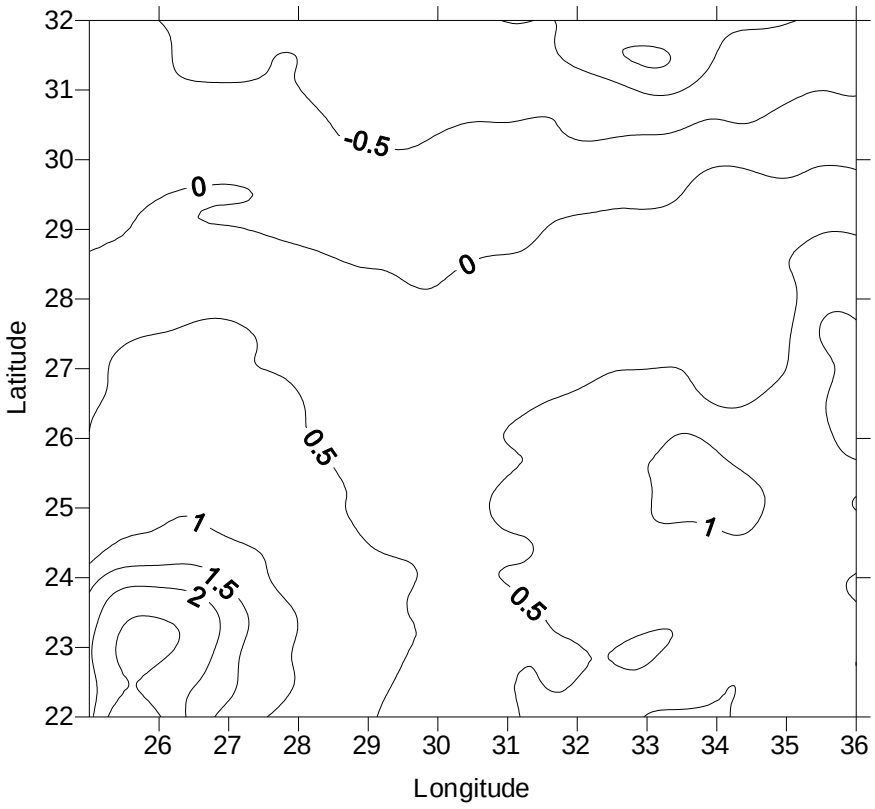


**Figure (4): Contour map of the difference between the EGM96 and the GFZ97 geoids for Egypt (Interval: 0.5 m)**

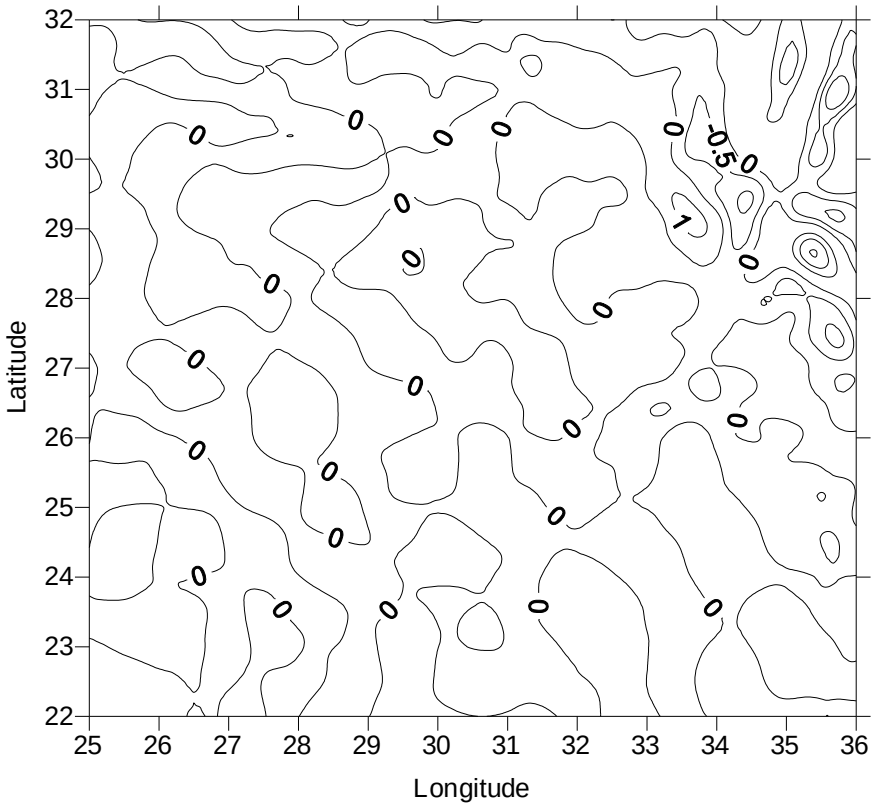


**Figure (5): Contour map of the difference between the EGM96 and the GPM98C geoids for Egypt (Interval: 0.5 m)**

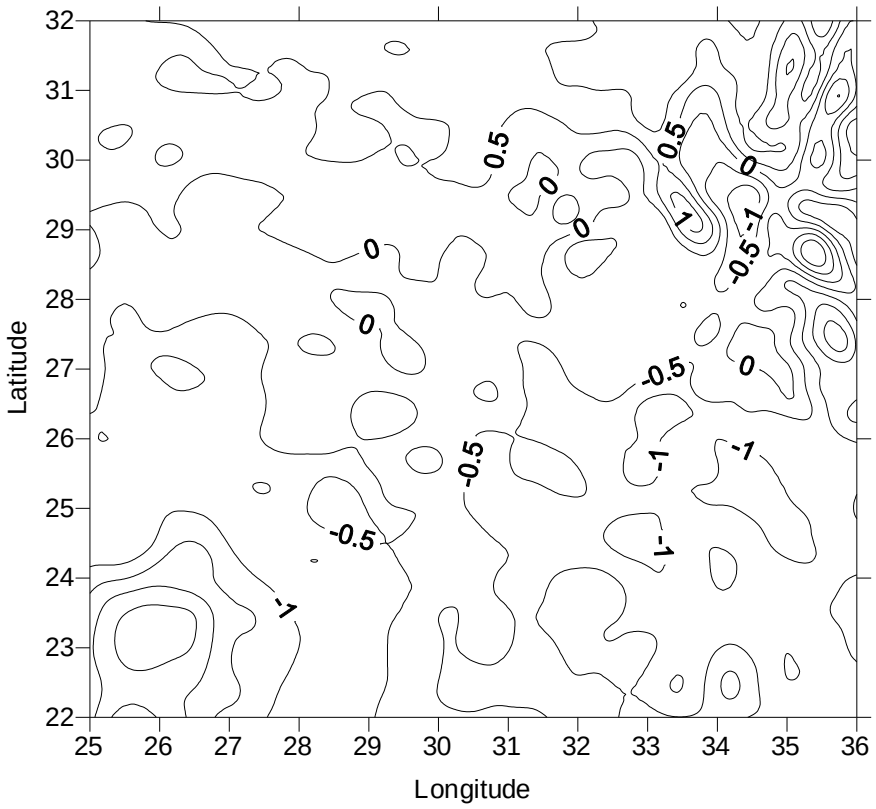


**Figure (6): Contour map of the difference between the GFZ97 and the GPM98C geoids for Egypt (Interval: 0.5 m)**

The residual free air anomalies and geoidal heights, pertaining to a specific harmonic models, are then a measure of how well that model recovers the low-medium spectral information in our area. The smoother are the residual features, the more efficient is the harmonic model in representing the low degree spectrum locally.

Table (2) shows a statistical comparison among the free air anomaly data and the residual free air anomalies resulting after the removal of the three models. It is clear that the three models have smoothed the gravity anomaly data in a similar manner in terms of the mean, standard deviation and RMS of the residuals. However, one could notice that the EGM96 model has a slightly better performance than the other two models. This conclusion also manifests itself in Table (3), which outlines the statistics of the relevant residual geoidal height observations. In that table, the residual geoidal heights, pertaining to the EGM96 model, give the minimum standard deviation and RMS values.

**Table (2): Statistics of the free air gravity anomalies reduced to the harmonic models (Unit: mgals)**

| Item | Mean | Std. Dev. | RMS | Min. | Max. |
|---|---|---|---|---|---|
| $\Delta g$ | -4.193 | 32.639 | 32.896 | -144.270 | 227.247 |
| $\Delta g$ – EGM96 | -0.440 | 27.612 | 27.605 | -155.505 | 206.327 |
| $\Delta g$ – GFZ97 | 0.572 | 27.901 | 27.897 | -163.293 | 209.835 |
| $\Delta g$ - GPM98C | -1.537 | 27.925 | 27.957 | -140.078 | 215.240 |

**Table (3): Statistical check of the harmonic models at 80 GPS-benchmarks (Unit: meters)**

| Item | Mean | Std. Dev. | RMS | Min. | Max. |
|---|---|---|---|---|---|
| N | 13.278 | 3.018 | 13.612 | 9.423 | 21.140 |
| N - EGM96 | 0.768 | 1.092 | 1.330 | -1.473 | 5.201 |
| N - GFZ97 | 0.945 | 1.207 | 1.527 | -1.589 | 5.321 |
| N- GPM98C | 0.669 | 1.160 | 1.333 | -1.502 | 5.070 |

## 5 Construction of the residual anomaly covariance functions

The isotropic covariance function, which is a function of the separation between the data points, describes the spatial variability of the local residual field under consideration. The important practical features of this function are the variance (covariance at zero distance), the correlation length, which corresponds to a positive covariance value that is equal to half the variance and the distance corresponding to the first zero covariance value, or simply the first zero. To estimate such an isotropic covariance function empirically at a spherical distance $\psi$, the product sum average of pairs of anomaly values, relevant to pairs of points having spacing $\psi$-$\Delta\psi/2 \leq \psi' \leq \psi+\Delta\psi/2$, was evaluated. Both $\Delta\psi$ and the $\psi$ increment were chosen to be 2 minutes of arc and 100 covariance values (at 100 $\psi$ values) were evaluated. Of course, such a function is dependent only on the spherical distances between pairs of stations, implying the invariance under a rotation of the data points group. An an-isotropic covariance function would be dependent on the positions of stations (Tscherning, 1999). The isotropic empirical covariance functions were estimated for the residual gravity anomalies relevant to the three models.

Figure (7) illustrates the trends of the three empirical covariance functions, while Table (4) shows the respective variances, correlation lengths and the first zeros. While the first zeros and correlation lengths, pertaining to the three models, are slightly different, the EGM96 shows relatively larger smoothing effect, in terms of the residual anomaly variance, than the GFZ97 and GPM98C models. Meissl (1971) and (Tscherning, 1974) show that the first zero point of a residual anomaly covariance function is a measure of how many spectral full degrees have been actually removed by a specific harmonic model. The relevant removed spectral degrees could be given by the $180^o/\psi^o$ rule of thumb (Meissl, 1971; Tscherning, 1974 and Rapp, 1977). Accordingly, and referring to Table (4), the EGM96, GFZ97 and GPM98C harmonic models could be judged to have removed degree and order 84, 83 and 84, respectively. These integer numbers are not far greater than the 70 satellite only recovered terms used for the combined solutions of the EGM96 (and implicitly, for the solution of the GPM98C) and GFZ97 harmonic models. This is an expected consequence for the absence of the local data in Egypt from the combined global solutions for these models.

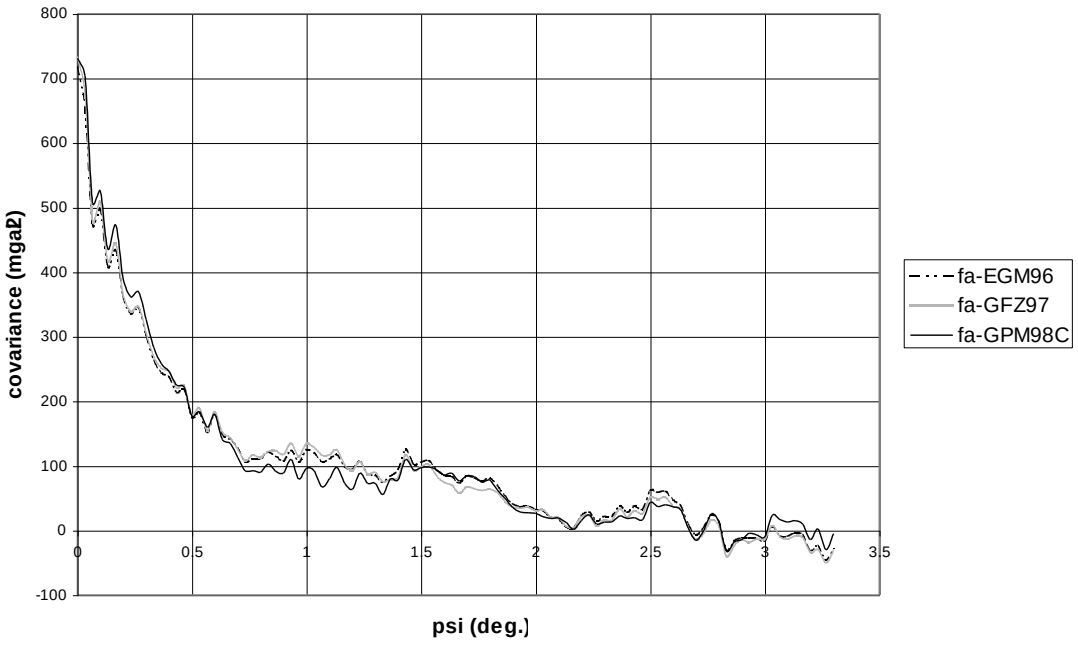


**Figure (7): The empirical covariance functions of the residual anomaly data sets relevant to the three models**

**Table (4): Main features of the empirical covariance functions of the residual gravity anomaly data pertaining to the three harmonic models**

| Reference field | Variance ($mgal^2$) | Correlation length | First zero |
|---|---|---|---|
| EGM96 | 717.673 | $0.200^o$ | $2.14^o$ |
| GFZ97 | 732.444 | $0.180^o$ | $2.17^o$ |
| GPM98C | 730.868 | $0.220^o$ | $2.14^o$ |

## 6 Free air geoid solutions by collocation using the models as reference fields

Least-squares collocation (LSC) is a prediction technique with a vital efficiency, since it provides minimum standard errors for the predicted signals based on the observational data and its noise. So, it was intended to utilize this technique to compute three 5'x5' free air geoid solutions for Egypt, relative to the WGS-84 ellipsoid, based on the harmonic models under study. In order to solve for a local geoid by the LSC, using the remove restore technique, it is important to formulate the model (analytical) covariance function that is best fitted to the residual anomaly empirical one in a least-squares sense. A modeled local covariance function that is consistent with the remove-restore of the relevant harmonic model is used to account for the removed spectrum. The modeled (analytical) covariance function is fitted to the residual anomaly empirical covariance function via a nonlinear 3-parameter iterative least-squares adjustment. The local isotropic anomaly covariance function model can be given as (Tscherning and Rapp, 1974 and Tscherning, 1993**)**

$$C(P,Q)= C(r,r',\psi)$$

$$=\sum_{n=2}^{k} c.\sigma^2_{neModel}.(R_b^2/rr')^{n+2}P_n(\cos\psi)+\sum_{k+1}^{\infty} A.(n-1)/(n-2).(n+24).(R_b^2/rr')^{n+2}.P_n(\cos\psi), \quad (3)$$

where

| | |
|---|---|
| $\psi$ | the spherical distance between the two points P and Q, |
| r | the geocentric radial distance of point P ≈ $R+H_P$, |
| r' | the geocentric radial distance of point Q ≈ $R+H_Q$, |
| R | the mean radius of the Earth, taken ≈ 6371 km, |
| $R_b$ | the radius of the Bjerhammar's sphere, |
| $\sigma^2_{neModel}$ | the $n^{th}$ anomaly error degree variance based on relevant coefficients' standard errors, |
| c | a positive unitless scale factor, |
| A | a positive constant ($mgal^2$), |
| k | the actual spectral degrees removed by the relevant harmonic model, and is equal in our case to 84 for both the EGM96 and GPM98C models and 83 for the GFZ97 harmonic model. |
| H | orthometric height of the respective point. |

As there is no available standard deviations for the GPM98C coefficients and for the sake of comparison, it was intended to proceed with a unified algorithm for modeling the analytical covariance functions of the residual anomalies, pertaining to the three harmonic models. Tscherning (1974) suggests that it is possible to consider the removed harmonic model errorless in the lower spectral band (from 0 to k), which has been actually removed from the local data by it. This is equivalent to assigning the respective error degree variances zero values, or the factor c in Eq.(3) is simply assumed zero. Hence, this strategy was followed in modeling the three covariance functions in the current study. Figure (8), (9) and (10) show the empirical covariance function and the associated fitted one for the residual anomaly data relevant to the EGM96, the GFZ97 and the GPM98C harmonic model, respectively.

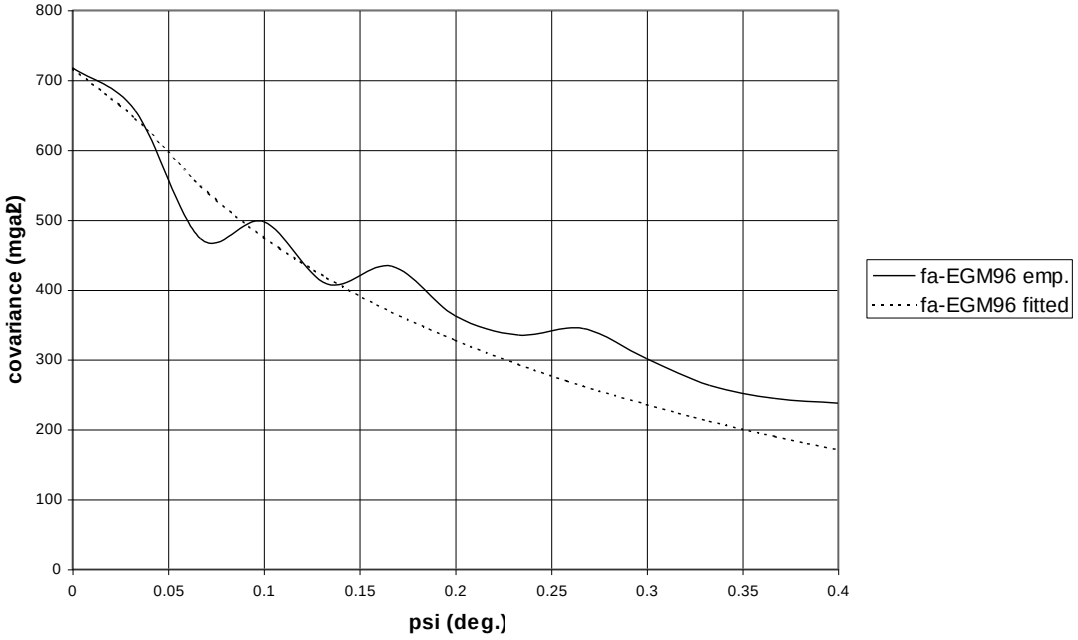


**Figure (8): The empirical and fitted covariance function of the residual anomalies relevant to the EGM96 model**

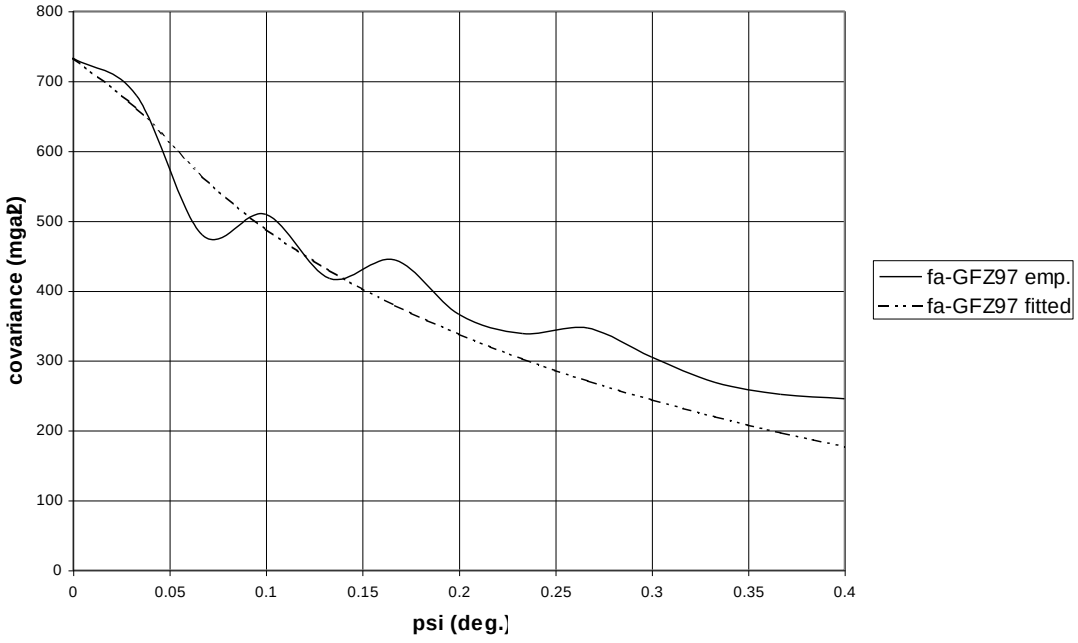


**Figure (9): The empirical and fitted covariance function of the residual anomalies relevant to the GFZ97 model**

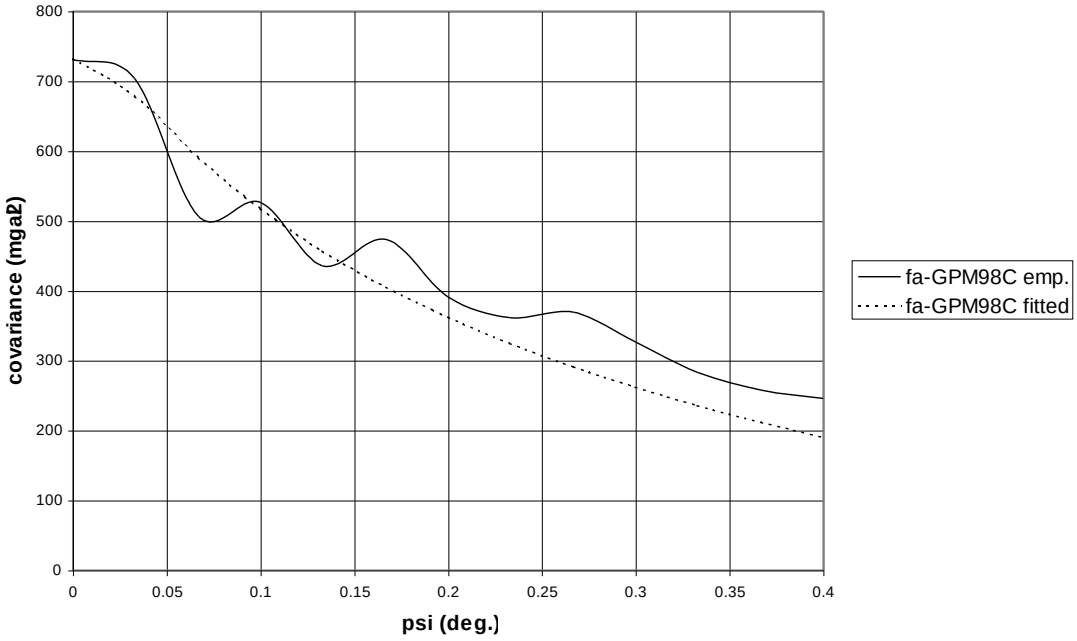


**Figure (10): The empirical and fitted covariance function of the residual anomalies relevant to the GPM98C model**

For each free air geoid solution, the respective residual anomaly data (along with the data noise), and the relevant three parameters of the fitted covariance function were input into the LSC solution. The immediate result of each solution were the respective 5'x5' residual geoid grid along with the corresponding error estimates, computed by the well known LSC expressions as follows

$$S = C_{st}.(C_{tt} + E_{tt})^{-1}. l, \quad (4a)$$

$$E_{ss} = C_{ss} - C_{st}(C_{tt} + E_{tt})^{-1} . C_{st}^{T}, \quad (4b)$$

with

| | |
|---|---|
| S | the vector of estimated (residual geoid) signals, |
| $C_{st}$ | the cross-covariance matrix between the signals S and the (residual gravity anomaly) observations l, |
| $C_{tt}$ | the covariance matrix of the (residual gravity anomaly) observations, |
| $E_{tt}$ | the error variance-covariance matrix of the (residual gravity anomaly) observations, |
| l | the vector of (residual gravity anomaly) observations, |
| $E_{ss}$ | the estimated error variance-covariance matrix of the estimated signals S, |
| $C_{ss}$ | the covariance matrix of the signals S. |

Then, using Eq.(1), the harmonic models' geoid components were then added back (restored) into the relevant residual geoid predictions at the grid nodes, in order to obtain the respective 5'x5' free air geoid solutions. Table (5) outlines the statistics of the various items of the resulting three free air geoid solutions. The statistics show slight differences among the error estimates, in terms of the mean, standard deviation and RMS. However, the EGM96-based solution seems to give the minimum

estimated geoid error, on the average. One could notice the similar statistics of the EGM96 and GPM98C-based final free air geoids, which are considerably different from those of the GFZ97-based solution. This is verified by Figures (11), (13) and (15), which show the final free air geoidal contour maps, based on the EGM96, the GFZ97 and the GPM98C harmonic model, respectively. The free air geoidal maps of Figures (11) and (15) are somewhat similar and different from that in Figure (13). On the other hand, Figures (12), (14) and (16) show the contour maps of the respective estimated geoid error grids. One could notice the similarity among the three free air geoid error maps.

**Table (5): Statistics of the items of the 5'x5' free air geoid grids using the different harmonic models as reference fields (Unit: meters)**

| Reference Field | Item | Mean | Std. Dev. | RMS | Min. | Max. |
|---|---|---|---|---|---|---|
| EGM96 | Free air geoid | 13.761 | 2.766 | 14.037 | 7.046 | 21.104 |
| | residual geoid | -0.043 | 1.023 | 1.024 | -2.968 | 5.677 |
| | Std. Error | 0.582 | 0.166 | 0.605 | 0.133 | 0.835 |
| GFZ97 | Free air geoid | 13.440 | 3.139 | 13.801 | 6.351 | 22.018 |
| | residual geoid | -0.048 | 1.059 | 1.060 | -3.191 | 5.799 |
| | Std. Error | 0.593 | 0.170 | 0.617 | 0.135 | 0.854 |
| GPM98C | Free air geoid | 13.766 | 2.804 | 14.048 | 6.559 | 21.354 |
| | residual geoid | -0.040 | 1.071 | 1.072 | -3.283 | 5.688 |
| | Std. Error | 0.599 | 0.179 | 0.625 | 0.124 | 0.877 |

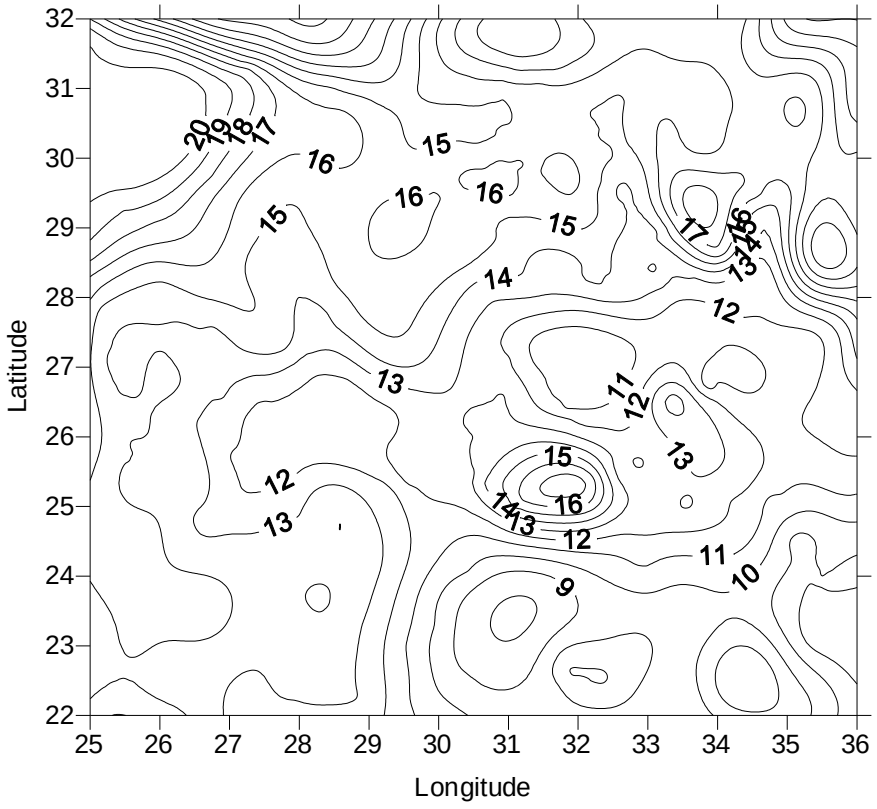


**Figure (11): Contour map of the free air geoid based on EGM96 (Interval: 1.0 m)**

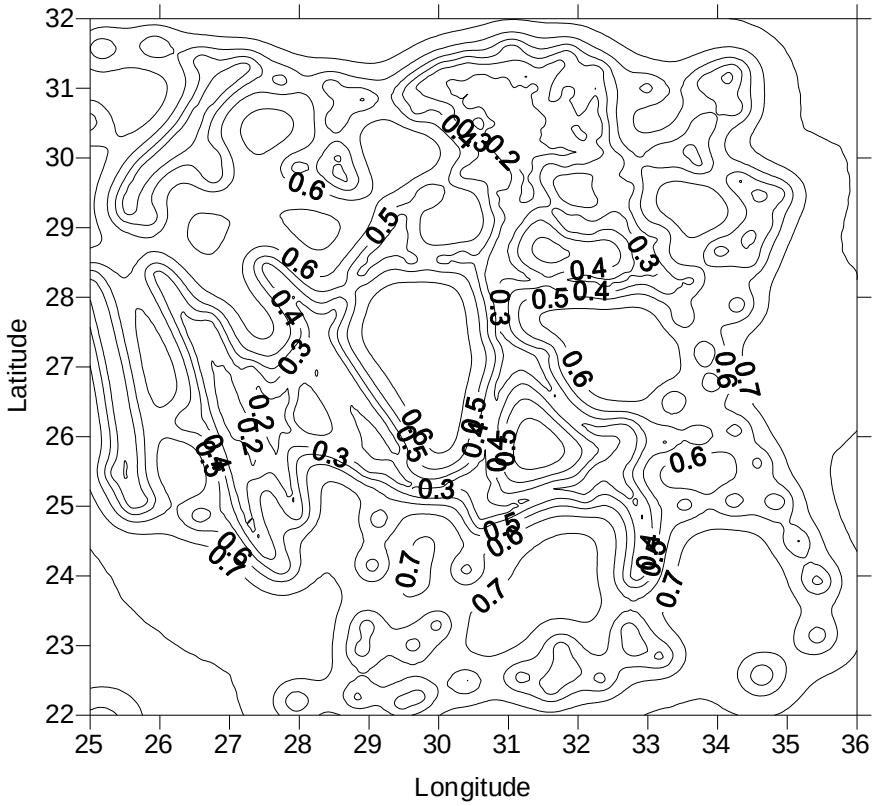


**Figure (12): Contour map of the estimated errors of the free air geoid based on EGM96 (Interval: 0.10 m)**

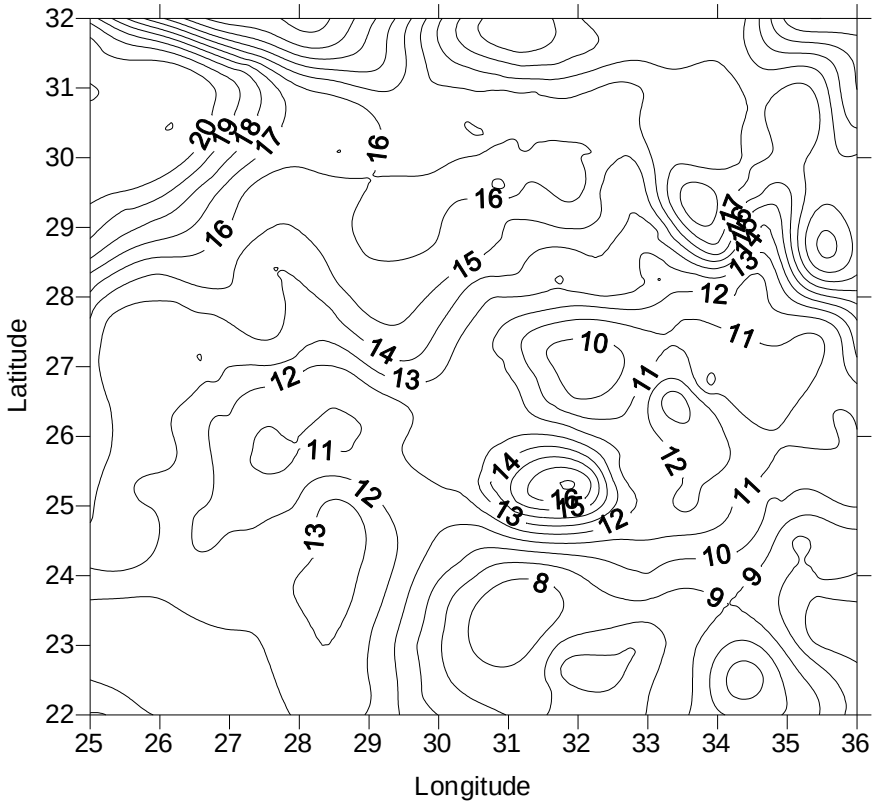


**Figure (13): Contour map of the free air geoid based on GFZ97 (Interval: 1.0 m)**

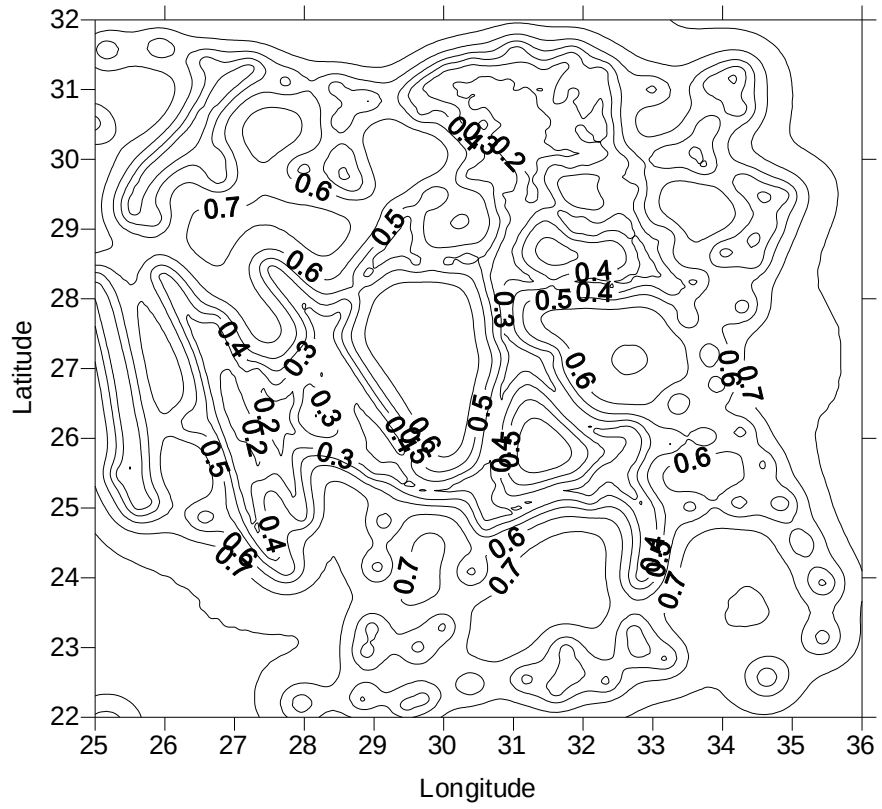


**Figure (14): Contour map of the estimated errors of the free air geoid based on GFZ97 (Interval: 0.10 m)**

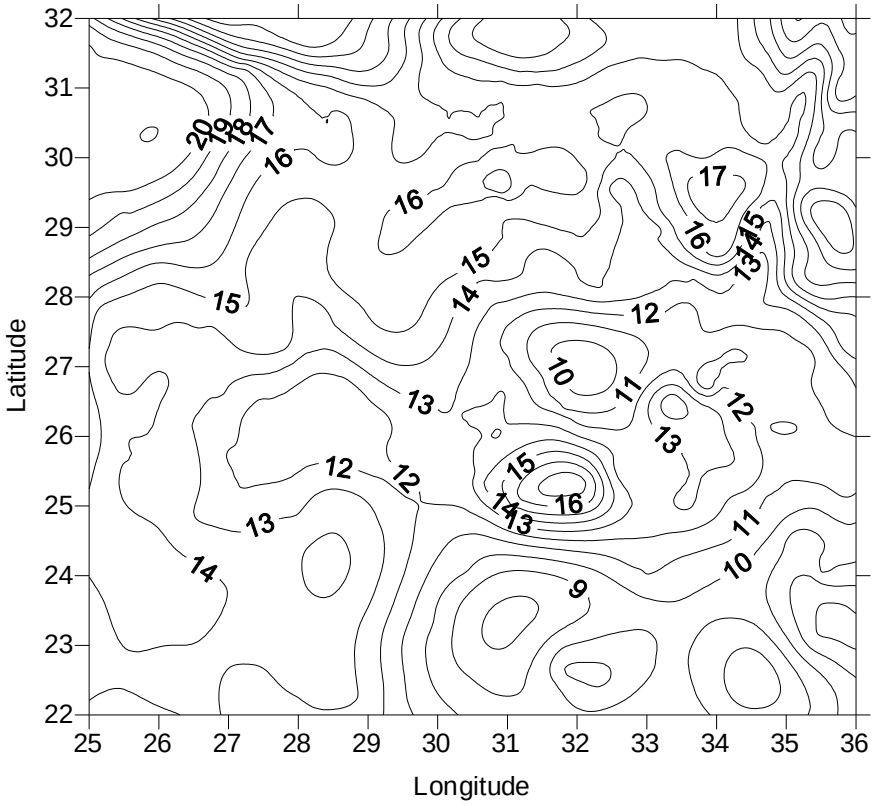


**Figure (15): Contour map of the free air geoid based on GPM98C (Interval: 1.0 m)**

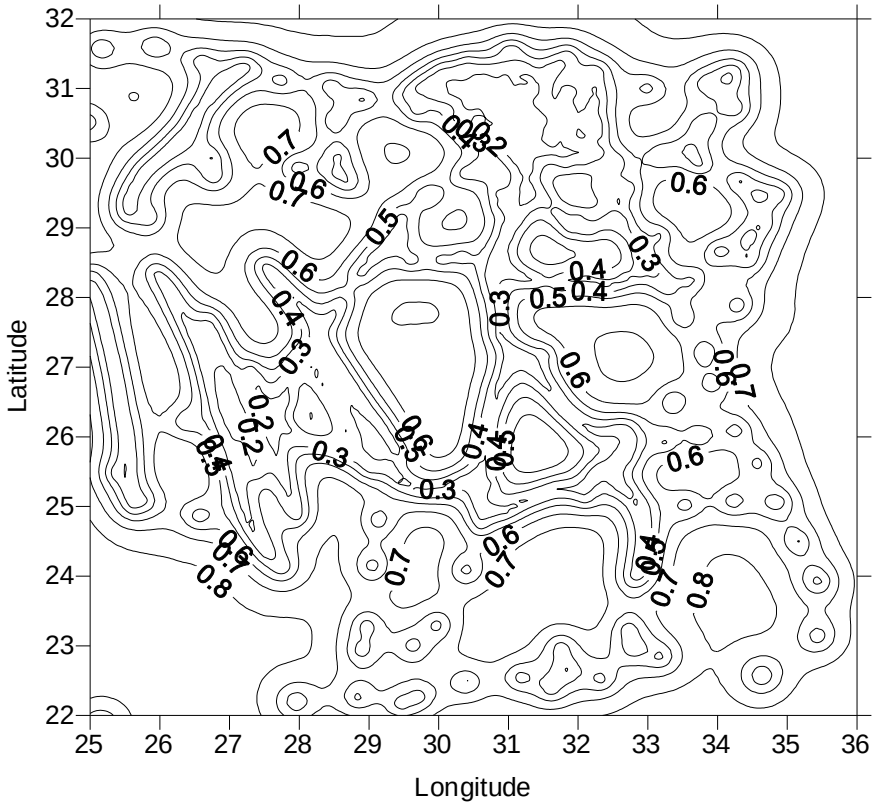


**Figure (16): Contour map of the estimated errors of the free air geoid based on GPM98C (Interval: 0.10 m)**

Finally, the three free air solutions were checked by the geoid height observations at the available 80 GPS-benchmarks, in order to give a statement about the external accuracy achieved by the three solutions. Table (6) gives the statistics of the relevant differences. Again, one could notice the slight difference between the accuracy of the EGM96 and the GPM98C-based geoid. Also, these two solutions have relatively better accuracy than that relevant to the GFZ97-based geoid solution.

**Table (6): Statistical check of the relevant free air geoid solutions at 80 GPS-benchmarks (Unit: meters)**

| Item | Reference Field | Mean | Std. Dev. | RMS | Min. | Max. |
|---|---|---|---|---|---|---|
| N(obs.)–N(pred.) | EGM96 | 0.317 | 0.931 | 0.978 | -3.649 | 3.133 |
| | GFZ97 | 0.543 | 1.038 | 1.165 | -3.635 | 3.426 |
| | GPM98C | 0.202 | 0.936 | 0.952 | -3.451 | 2.883 |

## 7 Concluding remarks

According to the current study, it can be concluded that none of the harmonic models under study has recovered the low-medium frequency features in an optimal manner for Egypt. All the investigated models have only recovered a number of spectral degrees that are nearly equal to the satellite only data inherent into them, thus not realizing their (nominal) maximum resolutions in the region under study. The

GPM98C behaves in most situations similar to the EGM96 harmonic model, as expected, since no local data were incorporated into either model. Both models have relatively different performance than the GFZ97 model. Having unreleased standard errors, it is better to use the GPM98C model in Stokesian local geoid solutions, since the covariance function modeling in LSC usually needs the error degree variances of the removed harmonic model. An insight into the obtained results shows that the EGM96 harmonic model has the best performance in Egypt, relative to the other two models.

Since the gravity anomalies and the other geodetic data have such great secrecy, which is not justified nowadays, and since there is no hope that the ESA would release such data for the international geodetic community to be used for computing future enhanced versions of global geopotential models, therefore it is highly recommended that all available gravity field data within the Egyptian region, performed by governmental and private surveying organization, be collected and used for tailoring the EGM96 geopotential model, in order to be more accurate and rather efficient for recovering the long-medium wavelength spectrum of the same field.

**References**

Amin, M.M. (1983): "Investigation of the Accuracy of some Methods of Astrogravimetric Levelling using an Artificial Test Area", Ph.D. Thesis in Physical Geodesy, Geophysical Institute, Czechoslovac Acad. Sci., Prague.

El-Tokhey, M. (1995): "Comparison of some Geopotential Geoid solutions for Egypt", Ain Shams University Scientific Bulletin, Vol. 30, No. 2: 82-101.

Gruber, T.; Anzenhofer, M.; Rentcsh, M. and Schwintzer, P. (1997): "Improvements in high-resolution gravity field modelling at GFZ. in Segawa, J.; Fujimoto, H. and Okub, S. (eds.) Gravity, Geoid and Marine Geodesy: 445-452.

Hanafy, M.S. (1993): "Global Geopotential Earth Models and their Geodetic Applications in Egypt", Ain Shams University Engineering Bulletin, Vol. 28, No.1: 179-196.

Lemoine, F.G.; Smith, D.E.; Kunz, L.; Smith, R.; Pavlis, E.C.; Pavlis, N.K.; Klosko, S.M.; Chinn, D.S.; Torrence, M.H.; Williamson, R.G.; Cox, C.M.; Rachlin, K.E.; Wang, Y.M.; Kenyon; S.C.; Salman, R.; Trimmer, R.; Rapp, R.H. and Nerem, R.S. (1996): "The Development of the NASA GSFC and NIMA Joint Geopotential Model", Proceedings paper for the International Symposium on Gravity, Geoid and Marine Geodesy (GRAGEOMAR 1996), The University of Tokyo, Tokyo, Japan, September 30-October 5.

Meissl, P. (1971): "A study of covariance functions related to the Earth's disturbing potential", Report No. 151, Department of Geodetic Science, The Ohio State University.

Rapp, R.H. (1977): "The relationship between mean anomaly block sizes and spherical harmonic representations", Journal of Geophysical Research, Vol. 82, No. 33: 5360-5364.

Shaker, A.; El-Sagheer, A. and Saad, A. (1997): "Which geoid fits Egypt better", Proceedings of the International Symposium on GIS/GPS, Istanbul, Turkey, September 15-19.

Smith, D.A. and Milbert, D.G. (1997): "Evaluation of the EGM96 Model of the Geopotential in the United States", IGeS Bulletin, No. 6: 33-46.

Tscherning, C.C. and Rapp, R.H. (1974): “Closed covariance expressions for gravity anomalies, geoid undulations and deflections of the vertical implied by anomaly degree variance models”, Report No. 208, Department of Geodetic Science, The Ohio State University.

Tscherning, C.C. (1974): “ A FORTRAN IV program for the determination of the anomalous potential using stepwise least squares collocation”, Report No. 212, Department of Geodetic Science, The Ohio State University.

Tscherning, C.C. (1993): “An experiment to determine gravity from geoid heights in Turkey”, GEOMED Report No. 3.

Tscherning, C.C. (1999): “Construction of an-isotropic covariance functions using Riesz-representers”, Journal of Geodesy, 73: 333-336.

Wenzel, G. (1998): “Ultra High Degree Geopotential Models GPM98A, B and C to Degree 1800”, Paper presented in Proceedings of the Joint Meeting of the International Geoid Commission, September 7-12, Trieste, Italy.